THE UNIVERSITY of EDINBURGH

Edinburgh Research Explorer

Synthesis, structure and spectroscopic properties of a new class of polymerisable nickel dithiolenes

OPEN ACCESS

Synthesis, Structure and Spectroscopic Properties of a New Class of Polymerisable Nickel Dithiolenes**

Simon Dalgleish,[1] Carole A. Morrison,[1] Derek S. Middlemiss,[2] Andrew R. Mount,[1] Anna Collins,[1]

Luca Pilia,[3] Angela Serpe,[3] M. Laura Mercuri,[3] Susan J. Roberts-Bleming,[4] Adam Charlton,[4]

Paola Deplano,[3,]* Patrick J. Murphy[4] and Neil Robertson[1,]*

[1]EaStCHEM, School of Chemistry, Joseph Black Building, University of Edinburgh, West Mains Road, Edinburgh, EH9 3JJ, UK.

[2]Department of Chemistry and WESTCHEM Research School, University of Glasgow, Glasgow, UK.

[3]Dipartimento di Chimica Inorganica e Analitica, S.S. 554, Bivio per Sestu, Monserrato, Italy.

[4]University of Wales, Bangor, Wales.

[*]Corresponding author; e-mail: neil.robertson@ed.ac.uk

Supporting information:
[†]Electronic supplementary information (ESI) available: Fig. S1 & S2: Crystal structures of 3 and 4 showing atom numbering scheme. Fig. S3: Solvatochromic studies of 3. Fig. S4: Optically transparent thin-layer electrochemistry (OTTLE) of 3 under reductive conditions. Fig. S5 & S6: Experimental and calculated UV/Vis/NIR absorbance spectra of 3 & 4. Fig. S7: Densities-of-states plots of 3 and 4. Fig. S8: Voltammograms of polymerisation of 3. Fig. S9 & S10: 1H NMR labelling scheme for 3 and 4. Table S1a, S2a, S1b & S2b: Selected experimental and calculated bond angles, experimental and calculated torsion angles of 3 and 4. Table S3: Selected transitions in the calculated and experimental spectra of 3 and 4. CCDC reference numbers 726849 and 726850. For ESI and crystallographic data in CIF or other electronic format see http://dx.doi.org/10.1039/B907028A

Abstract

The synthesis, structure and spectroscopic properties of a new class of asymmetric nickel dithiolene complex containing pendent thiophene units [Ni(R$_2$pipdt)(b-3ted)] are described {R = Bz (**3**), ^{i}Pr (**4**); pipdt = piperazine-3,2-dithione; b-3ted = *bis*(3-thienyl)-1,2-ethylenedithiolene}. X-ray crystallography of both neutral species shows planar nickel dithiolene units and the thiophene groups twisted out of the molecular plane, with the R group having a large effect on the packing structure. DFT geometry calculations show good agreement with experimental data for **3** and **4** and confirm that the low energy absorption, assigned to a HOMO→LUMO transition, is inter-ligand charge-transfer in character. Solid state calculations show greater band dispersion in **4**, which corresponds to a closer packing in the crystal lattice. Cyclic voltammetry of both complexes displays three reversible processes, corresponding to an interconversion between cationic, neutral, anionic and dianionic species, with tuning of the redox potentials by variation of the R group. Electrochemical polymerisation of **3** shows incorporation of intact dithiolene units into a polymer film with redox functionality similar to that of the monomer, whereas co-polymerisation of **3** with thiophene yields a highly conductive film with redox functionality similar to polythiophene and enhanced absorption across the near IR.

Introduction

Nickel dithiolenes[1] have found widespread application within the field of materials chemistry. Their conductive properties have been tuned to develop semiconductors,[2] metals and superconductors,[3, 4] whist their optical properties have been employed for Q-switching near-infrared (NIR) lasers[5, 6] and the development of non-linear optic (NLO) materials.[7] Long excited state lifetimes and highly-tuneable absorption profiles also offer the possibility for their incorporation into photovoltaic devices.[8] It is because of this range of applications, combined with their high thermal and photochemical stability,[5] that nickel dithiolenes have remained under intensive investigation for over 40 years in an effort to prepare multifunctional dithiolene complexes.[9] Beyond academic interest, an interplay between their optical, magnetic and conductive properties might lead to the development of optoelectronic or magnetooptic materials for novel device construction.

Asymmetric dithiolene complexes (where L≠L′) are desirable targets as the frontier orbitals may become localised on different ligands, and thus a HOMO→LUMO transition would have inter-ligand charge-transfer (ILCT) character – a requirement for second-order NLO chromophores.[10] Such molecules generally have improved solubility in common organic solvents due to their permanent ground state dipole and, as such, thin-film formation by cheaper solution methods can be achieved. The bonding motif in unsymmetrical nickel *bis*-dithiolene systems can be thought of as being [Ni(II)(dithione)(dithiolate)] in character, where the electron donating dithione pushes electron density towards the electron withdrawing dithiolate, leading to their being termed '*push-pull*' complexes.[7] Asymmetric nickel *bis*-dithiolenes containing the R$_2$pipdt ligand have previously been reported.[11, 12] Their low energy absorption, as well as their packing structure and solid state

properties, can be easily tuned by variation of the R group. Such asymmetric complexes allow fine tuning of the structural and electronic properties through one ligand, whilst maintaining the functionality imposed by the other.[12, 13]

Incorporation of pendent thiophene groups can afford materials that combine the properties of polythiophene, such as conductivity, flexibility and good stability,[14] with the optical properties of the dithiolene.[15] These materials can be grown directly onto flexible substrates by electrochemical or solution methods to form flexible devices such as organic light emitting diodes and photovoltaics.[16] Symmetric nickel *bis*-dithiolenes containing pendent thiophene groups have previously been reported by ourselves and others,[17-19] and electrochemical polymerisation of these complexes has been shown to produce films through covalent linkage of the thiophene groups. Pickup *et al.* showed polymerisation of [Ni(b-2ted)$_2$] gave conducting films with redox functionality similar to the monomer,[19, 20] whereas Murphy *et al.* showed polymerisation of [Ni(b-3ted)$_2$] yielded an insulating film under similar conditions.[17] The observed poor conductivity in [Ni(b-3ted)$_2$] was thought to be due to low structural regularity, caused by excessive cross-linking of the thiophene groups. Films formed by a co-polymerisation of [Ni(b-3ted)$_2$] with thiophene, however, showed greatly improved conductivity with redox functionality similar to that of polythiophene.[17]

In this paper we report the synthesis and characterisation of two electrochemically-polymerisable asymmetric nickel *bis*-dithiolene complexes. These have been designed with controlled numbers of polymerisable thiophene units per molecule to enable formation of high-quality conducting films and to allow straightforward tuning of the optical properties of these molecules and films.

Results and Discussion

Full experimental details for the syntheses of the b-3ted ligand precursor **1**[21] and R$_2$pipdt (R = Bz **2a** R = ^{i}Pr **2b**) have previously been reported.[7, 11, 22, 23] Both **3** and **4** were synthesised by analogous routes: **1** was treated with sodium methoxide in dry methanol under a nitrogen atmosphere, and to this was added a mixture of NiCl$_2$.6H$_2$O and R$_2$pipdt in methanol (Scheme 1). The crude product precipitated immediately as an air stable green suspension which was filtered and washed with cold methanol. The precipitate was dissolved in DCM and passed through a silica plug to remove insoluble symmetric dithiolene salts and the solvent removed to afford pure product as a green precipitate. Crystallisation by slow diffusion of ether into DMF yielded analysable crystals of each target materials as dark green needles.
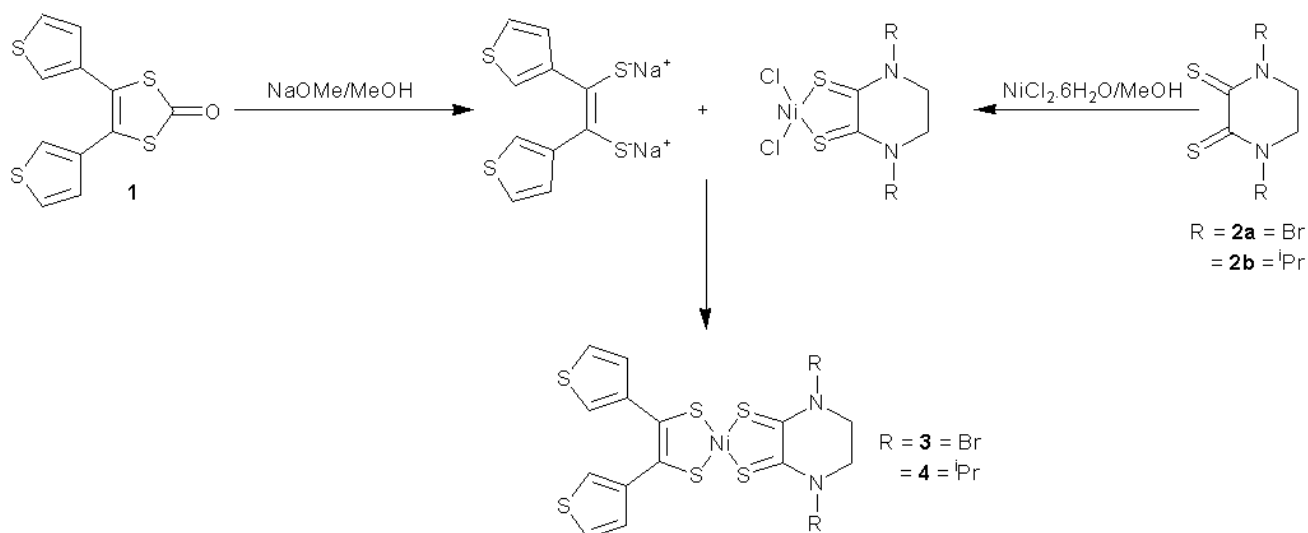
Scheme 1. Synthetic route toward [Ni(R$_2$pipdt)(b-3ted)].

Both **3** and **4** crystallised with the central Ni atom coordinated by four S atoms in an approximately square planar environment, with Ni-S coordination bonds broadly similar on both sides of the complex. Within the central NiS$_4$C$_4$ core, the C-C bond on the b-3ted ligand is significantly shorter than that of the R$_2$pipdt (0.123(5) Å for **3** and 0.129(4) Å for **4**) and the C-S bonds are shorter on the R$_2$pipdt than the b-3ted (0.068(3) Å for **3** and 0.059(3) Å for **4**). These results are consistent with previous studies of '*push-pull*' complexes[7, 12] and confirm the C-S π* and C-C π nature of the frontier MOs on the ligands.[7] A comparison of the C-S bond lengths with those reported for free ligand analogues of R$_2$pipdt[12] and b-3ted,[24] shows good agreement, which confirms the [Ni(dithione)(dithiolate)] nature of the complexes (Fig. S1 & S2; Tables S1 & S2, ESI†).

Examination of the packing structure of both complexes shows the R group to have a large effect on how the molecules arrange in the lattice. **3** forms a herringbone arrangement with an interplanar distance of 4.172 Å (Fig. 1), whereas **4** forms head-to-tail puckered sheets with an interplanar distance of 3.949 Å (Fig. 2). Both complexes display a large interplanar distance due to the out-of-plane twist of the thiophene groups; in addition, the bulk of the Bz group prohibits close packing of the NiS$_4$C$_4$ cores in **3**. Some disorder was observed for **3** due to a rotation of the C(4)-C(6) bond. This gave a 65% probability of a thiophene conformation different to that observed in **4**. This disorder may be due to the increased bulk of the benzyl groups and larger inter-planar distance resulting in poorer orbital overlap of the thiophene groups between molecules.
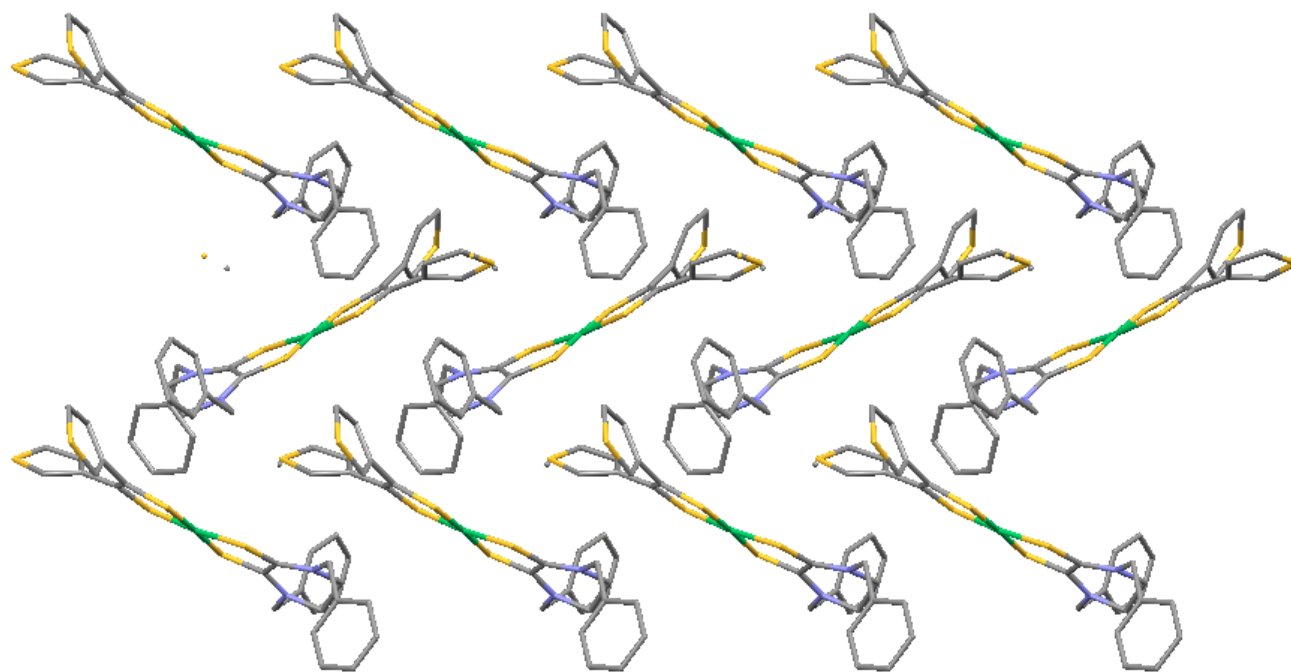
Figure 1. X-ray packing structure of **3** showing the herringbone packing arrangement.[25]
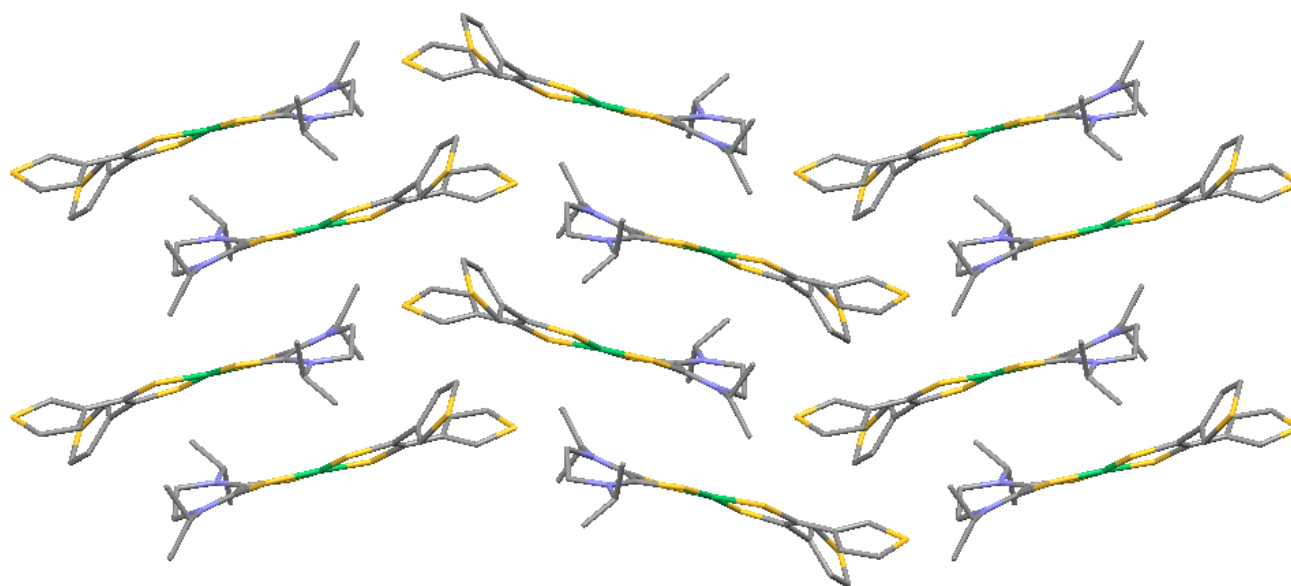
Figure 2. X-ray packing structure of **4** showing the head-to-tail puckered sheet packing arrangement.[25]

Spectroscopic Studies

UV/Vis/NIR spectroscopy of **3** and **4** in DMF show an intense peak in the UV region and a single peak in the NIR region [940 nm (10,638 cm^{-1}) and 928 nm (10,776 cm^{-1}) for **3** and **4** respectively] (Fig. S5 & S6, ESI†). It is this low energy absorption that provides the most information about the electronic structure of these complexes as it is attributed to a HOMO→LUMO transition that is predominantly LL′CT in character.[10] This is caused by the unbalanced contribution of the two ligands to the frontier orbitals. The value of λ_{max} is greater for **3** than **4**, indicating a smaller HOMO-LUMO gap, which is in agreement with conclusions drawn from electrochemical studies (*vide infra*). Spectra were obtained in a range of solvents and both complexes show negative solvatochromic behaviour. This suggests that more polar solvents stabilize the ground state of both **3** and **4** to a greater extent than the excited state, and thus both complexes have a more pronounced dipole moment in the ground state (Fig. S3, ESI†).

To further characterise the nature of the frontier orbitals, the change in the absorption spectrum of **3** upon reduction and oxidation was studied in 0.1 M TBABF$_4$/DMF at -40 °C. Complete reduction was achieved by holding the potential at -0.8 V until no further change in the absorption profile was observed (Fig. S4, ESI†). The NIR band collapsed as a new band at lower energy grew in at 1028 nm (9,728 cm^{-1}). A reduction in the intensity of the UV band was also observed as a shoulder to the existing peak grew in at 365 nm (27,397 cm^{-1}). The neutral species could be rapidly and reversibly regenerated by holding the potential at +0.1 V. Oxidation of the neutral species at +0.8 V again resulted in the collapse of the NIR band and the formation of a lower energy transition at 1294 nm (7,728 cm^{-1}). This species proved unstable over the course of the experiment as the peak gradually collapsed to the baseline, followed by a steady decrease in the intensity of all other bands. This experiment confirms the stability of the anionic complex, but suggests that cationic species is affected by processes of unknown nature (e.g. precipitation or decomposition), which reduces its stability over long periods in solution (*vide infra*). The spectro-electrochemical experiments show that the switching of redox states of these complexes generates distinct electronic absorptions in the NIR. This behaviour makes these materials of interest as polyelectrochromic NIR dyes for electrochromic devices.[26, 27]

Computational Studies

Ab initio molecular orbital calculations (see Experimental section for details) were performed on **3** and **4** to confirm that, although the frontier orbitals are spread over the whole molecule, the HOMO is largely b-3ted in character, whilst the LUMO is almost entirely located on the R$_2$pipdt (Fig. 3). Geometry optimisation of both complexes showed excellent agreement of the bond lengths with the observed X-ray data, however, the degree of planarity in the central NiS$_4$C$_4$ core was underestimated (Tables S1 & S2, ESI†). These deviations away from X-ray data may be due to constraints imposed by the crystal lattice as the calculations were run on isolated molecules. Following optimisation, information regarding the electronic excitation properties for **3**

and **4** were sought using time-dependent density functional theory (TD-DFT). Calculations were carried out using the polarisable continuum model of DCM (ε = 8.93), as previous computational studies of other charge-transfer systems in the gas phase have been shown to drastically underestimate the energy of the transitions.[28] The calculated contributions to the low energy band in **3** were shown to be 54 % HOMO→LUMO and thus predominantly LL′CT in character, with a contribution from the HOMO-3→LUMO transition. The low energy band in **4** was 65 % HOMO→LUMO in character, with only a very minor contribution from HOMO-3→LUMO. The calculations overestimated the energy of all the observed transitions for both **3** and **4** (~1550 cm^{-1} for the low energy transition), but showed good relative correlation between the two complexes (Table S3, ESI†). A transition from the HOMO-2→LUMO was calculated but not observed for both complexes which was predominantly MMLL′CT in character [543 nm (18,416 cm^{-1}) for **3** and 528 nm (18,927 cm^{-1}) for **4**]. If the energy of this transition was also underestimated by the calculation, it may account for the weak shoulder peak of the low energy transition in the observed spectra of both complexes (Fig. S5 & S6, ESI†). The polarisable continuum model models non-specific solvation and does not account for other, more complex, effects that occur in real systems, such as specific solvent coordination.
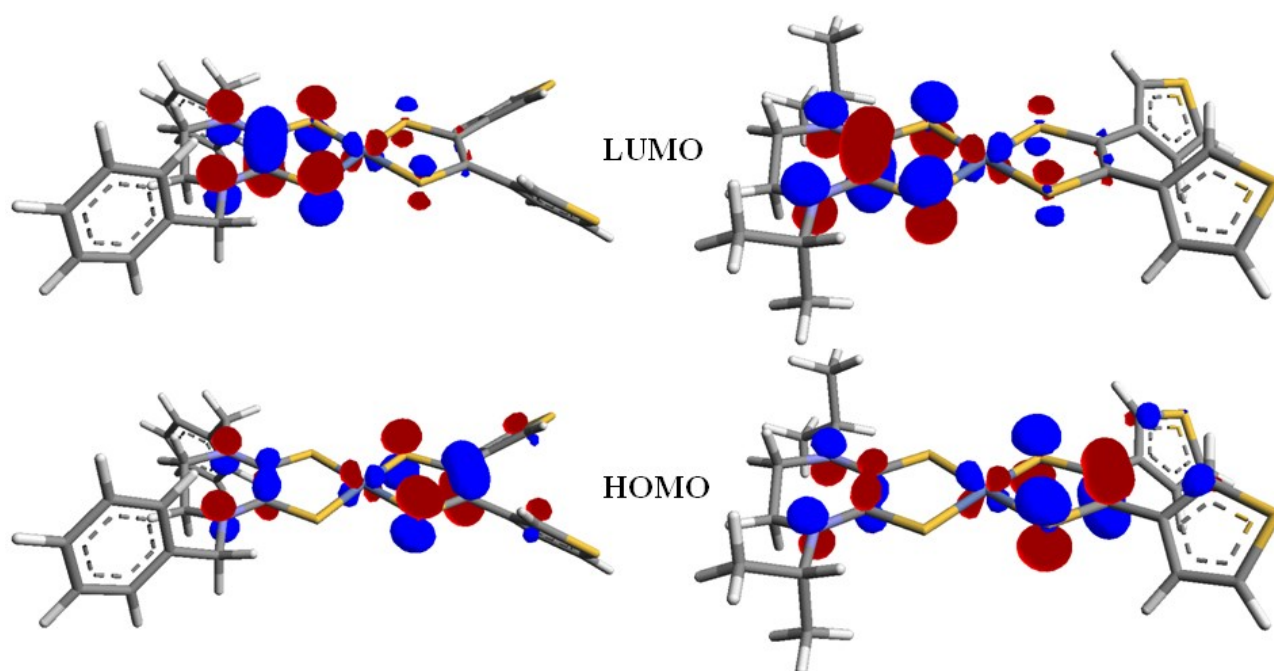
***Figure 3.*** Frontier molecular orbitals of **3** and **4**.

In order to explore the bulk properties of these complexes in the solid state, DFT calculations were performed using the CRYSTAL06[29] code to investigate the degree of molecular overlap and develop a band structure for both materials. Visualisation of densities-of-states plots showed that the calculated distribution of the frontier

orbitals in the crystal structures was in agreement with the calculations performed on isolated molecules (Fig. S7, ESI†). The band dispersion plots, shown along pathways cutting through symmetry significant k-points in reciprocal space, are given in Figure 4. The maxima and minima of the valence and conduction bands, respectively, lie upon the same k-vector for both **3** and **4**, and thus both complexes are calculated to have a direct band gap. For **3** the HOMO and LUMO bands appear at around -4.5 eV and -2.5 eV, respectively, with a band gap of *ca*. 1.54 eV (805 nm). For **4**, the HOMO and LUMO bands are around -4.0 eV and -2.5 eV, respectively, and the calculated band gap is slightly larger at *ca* 1.59 eV (779 nm). The relative size of the band gap is thus calculated to be the same in the solid-state, compared to the experimentally determined HOMO-LUMO gap from UV/Vis/NIR studies. However, a greater degree of band dispersion is calculated for **4**, which in turn can be attributed to the closer packing of the NiS_4C_4 cores in the crystal lattice. The k-point axis of largest dispersion in **4** (denoted C) corresponds to a vector parallel to the a-axis in the crystal lattice and provides the closest contact between the NiS_4C_4 cores.
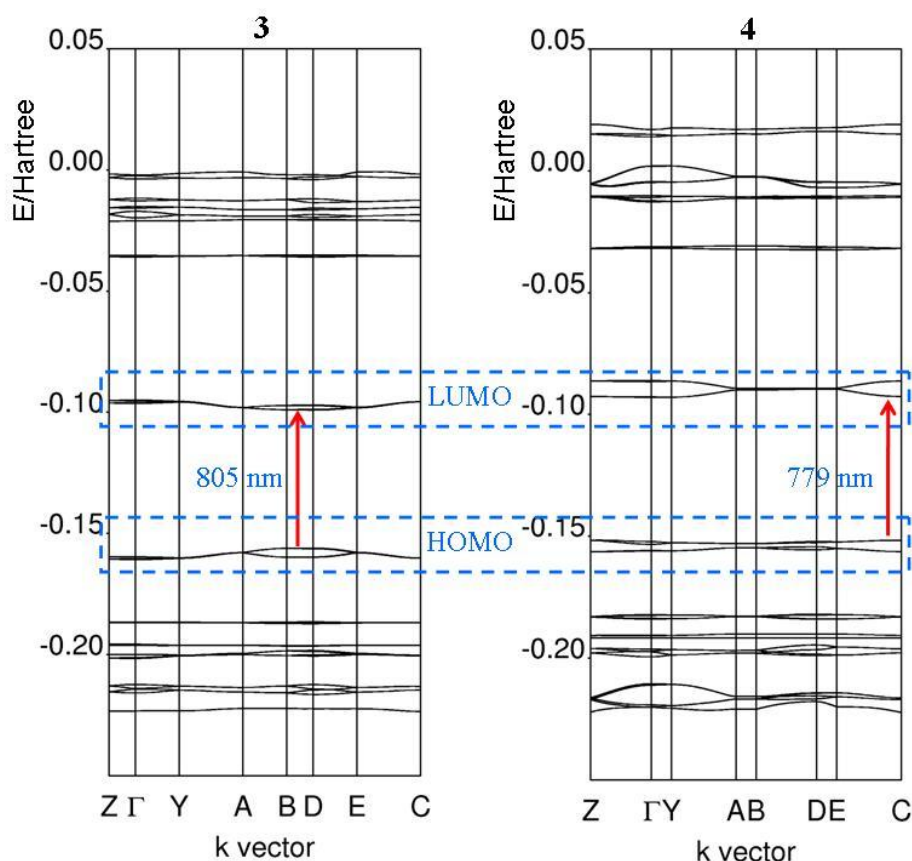
Figure 4. Band structure of **3** and **4** showing the frontier orbitals using the CRYSTAL06 code.

Electrochemical Studies

3 and **4** were each studied by cyclic voltammetry in a solution of 0.1 M TBABF$_4$ in DMF (Fig. 5). Both complexes show three electrochemically reversible one-electron redox processes (confirmed by the peak shapes and the linear plots of current vs. the square root of scan rate). The two processes at negative potentials were assigned to the [MLL′]$^{2-/1-}$, [MLL′]$^{1-/0}$ redox processes, whilst the reversible process at positive potentials was assigned to [MLL′]$^{0/1+}$, indicating the formation of a stable cation under cyclic voltammetric analysis (scan rates sampled at intervals between 10-1000 mVs^{-1}). Two irreversible peaks were seen above +1 V, and were assigned to sequential oxidation of the thiophene groups [*vide infra* (Table 1)].
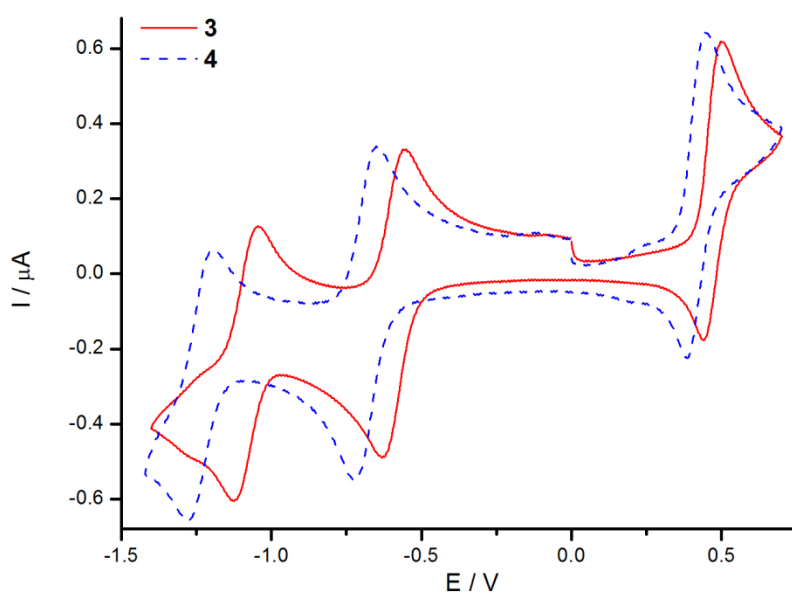
Figure 5. Cyclic voltammetry (100 mVs^{-1}) of **3** and **4** showing three reversible redox processes, tuneable through the R-group. The starting potential was 0.0 V and the initial direction of the sweep was to more positive potentials.

Table 1. Redox potentials of the free ligands **2a** and **2b**, complexes **3** and **4** and a poly-**3** coated platinum electrode. All processes are reversible, unless otherwise stated; *irreversible, §quasi reversible.

Name	E$^1_{1/2}$ / V	E$^2_{1/2}$ / V	E$^3_{1/2}$ / V	E$^4_{1/2}$ / V	E$^5_{1/2}$ / V
2a	-	-1.24	+1.13*	-	-
2b		-1.40§	+1.01*		
3	-1.09	-0.59	+0.46	+1.11*	+1.38*
4	-1.26	-0.68	+0.42	+1.05*	+1.38*
Poly-3	-0.68*	+0.02	+0.40	+0.98*	+1.18*

Each redox process occurs at a more positive potential for **3** than **4**, thus the nature of the R group is shown to affect the redox behaviour of the dithiolene core. Greater variation in the redox processes at negative potentials ($\Delta E^1_{1/2} = 0.17$ V, $\Delta E^2_{1/2} = 0.09$ V) than at a positive potential ($\Delta E^3_{1/2} = 0.04$ V) lends experimental weight to the computational data which show the LUMO to be predominantly located on the R_2pipdt. This is in agreement with UV/Vis/NIR data and agrees with previous work on electronically analogous systems containing the R_2pipdt ligand,[7, 11] which concluded that the more electron rich ^{i}Pr$_2$pipdt raises the energy of the LUMO more than that of the HOMO.[7]

In order to demonstrate the potential for this new class of complex to be incorporated into conducting films, the electrochemistry of **3** was studied at higher concentrations. This complex was chosen due to its superior solubility in common organic solvents and its greater optical absorbance in the NIR range, thus making it easier to process and characterise. Concentrations of between 5 and 10 mM of monomer in a solution of 0.3 M TBABF$_4$ in DCM were used, due to the observed solubility of the deposited films in DMF. Potential cycling between +0.87 and +1.47 V to initiate oxidation of both thiophene groups resulted in an initial drop in current after the first scan, followed by a steady increase that continued for many cycles (Fig. S8, ESI†). This is indicative of the deposition of a conducting film. By comparison with previous studies,[17] it is assumed that the electrochemical process observed in this range is the covalent linking of the thiophene groups at the α-position, resulting in polymeric growth on the electrode surface.

Cycling of this film between +1.00 and -1.00 V in monomer free electrolyte solution initially showed none of the redox processes observed for the monomer, but on cycling to greater potentials (+1.50 and -1.30 V), three redox processes emerged at -0.68, +0.02 and +0.40 V and remained over many cycles (Table 1, Fig. 6). On comparison with the cyclic voltammetry of the monomer, the redox process at positive potential (E^3) appears largely unchanged, whilst the redox processes at negative potentials are shifted to more positive potentials (~400 mV for E^1 and ~600 mV for E^2). More facile reduction may be due to stabilisation of the LUMO upon polymerisation. Alternatively, these differing shifts may reflect the the need to incorporate a different counterion upon reduction compared with oxidation. A conditioning process seems to be required to activate the film. We propose that this may be the result of film restructuring to mitigate against poor initial counter ion transport through the film.[30] The initial potential cycling and film formation experiment should lead to the deposition of neutral or cationic film products with associated BF$_4^-$ counterions. However, film cycling to generate reduced species requires bulky TBA$^+$ film transport to preserve electron neutrality. Cycling the film to these negative potentials enables film restructuring to allow such ion transport.
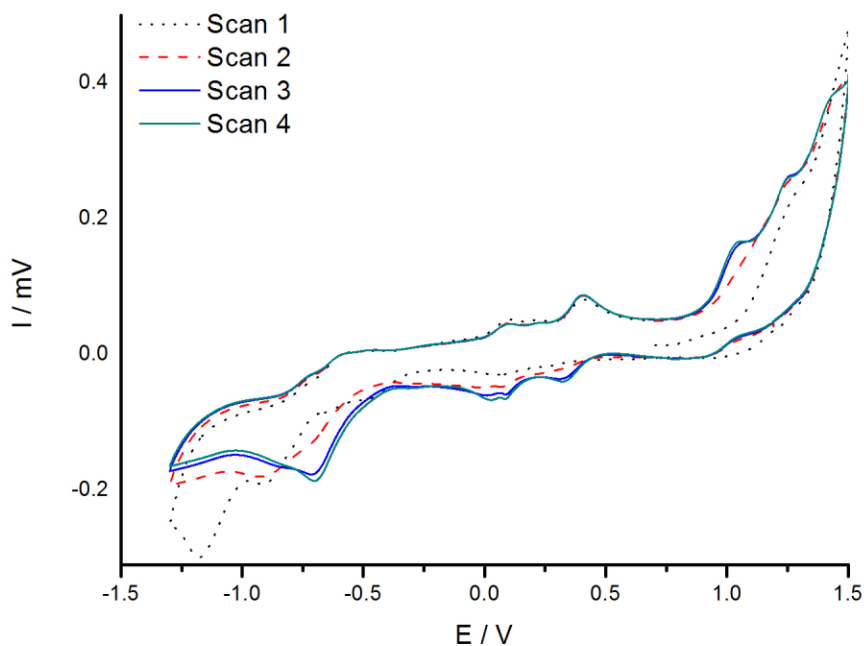
Figure 6. Cyclic voltammetry (100 mVs^{-1}) of a poly-**3** coated platinum electrode in 0.3 M solution of TBABF$_4$ in DCM.

Films were grown on fluorine-doped tin oxide (FTO) coated glass electrodes to enable analysis of the deposited films (gold in colour) by UV/Vis/NIR spectroscopy (Fig 7). Initial analysis was complicated by a broad absorption over the entire spectral range; however, by washing the electrodes in DMSO, the nature of the film could be ascertained. For the soluble portion, the absorption around 250 – 500 nm is indicative of thiophene linkage,[20] however, the comparative weakness of this absorption at longer wavelengths suggests that the chain lengths of the dissolved portion were short. Unequivocal evidence for incorporation of the intact dithiolene complex moieties was demonstrated by the characteristic near-IR absorption around 950 nm. The insoluble portion of the film showed, in comparison, stronger absorption across the 400 – 800 nm region, consistent with lower solubility due to longer polythiophene chains. In addition, a very distinct near-IR absorption was observed centred around 1550 nm, considerably red-shifted (by 4360 cm^{-1}) from the absorption of **3**. This red-shift may be due to strong interaction between dithiolene complexes and the polythiophene backbone or due to absorption by ionic dithiolene units (*vide supra*) stabilised in the solid-state system. In either case, such a pronounced red-shift is indicative of an interplay between the conductive polythiophene backbone and the optically active dithiolene unit.
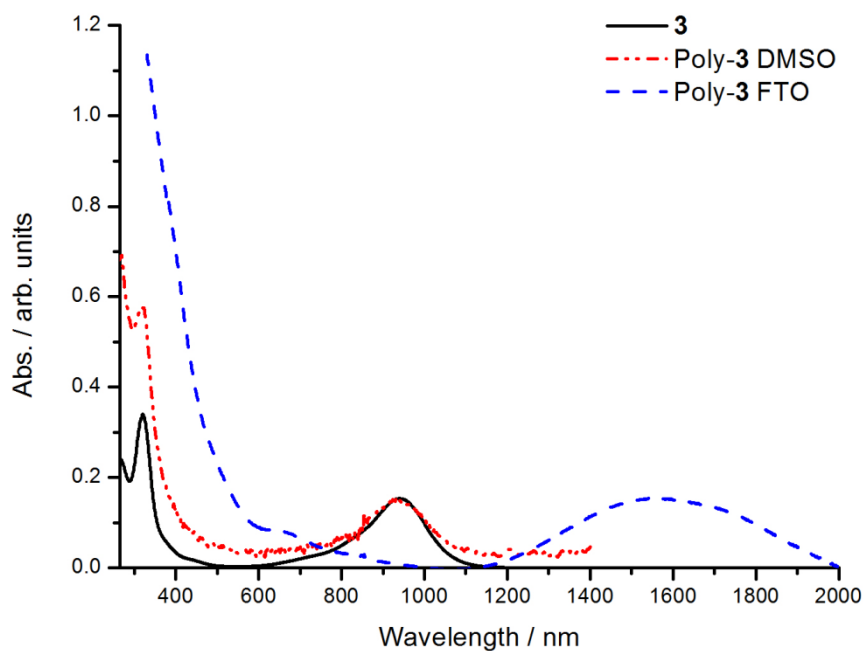
Figure 7. Normalised UV/Vis/NIR spectra of **3** in DMSO, poly-**3** on FTO and dissolved poly-**3** in DMSO.

In an effort to further explore the structural and electronic properties of films containing **3**, hybrid films of **3** and thiophene were produced. Adding 10 mM of thiophene to the monomer solution and potential cycling between +2.37 and -0.23 V resulted in the deposition of a highly conducting film. This film displayed similar redox behaviour to polythiophene and did not show any of the redox processes observed in the dithiolene complex, which were possibly obscured by the dominant polythiophene processes. The deposited film was brown in colour and insoluble in DMSO. UV/Vis/NIR spectroscopy of films grown on FTO coated glass electrodes showed a broad absorption over the entire NIR range. On comparison with the spectrum of a polythiophene film grown under identical conditions, distinct differences in the spectra can be observed. The hybrid film showed intense NIR absorptions centred around 950 nm (shoulder) and 1400 nm (peak) (Fig. 8), that were absent from the polythiophene film. These can reasonably be attributed to incorporated dithiolene units with both these low-energy absorptions comparable to those observed in the soluble and insoluble portions respectively of the homopolymer of **3**. The intermediate red-shift of the lowest energy NIR absorption to 1400 nm, rather than 1550 nm for the homopolymer suggests that, by careful stoichiometric control, the NIR absorption profile, as well as the conductive properties, of a hybrid polymeric film containing such complexes might be tuned over a wide range of wavelengths.
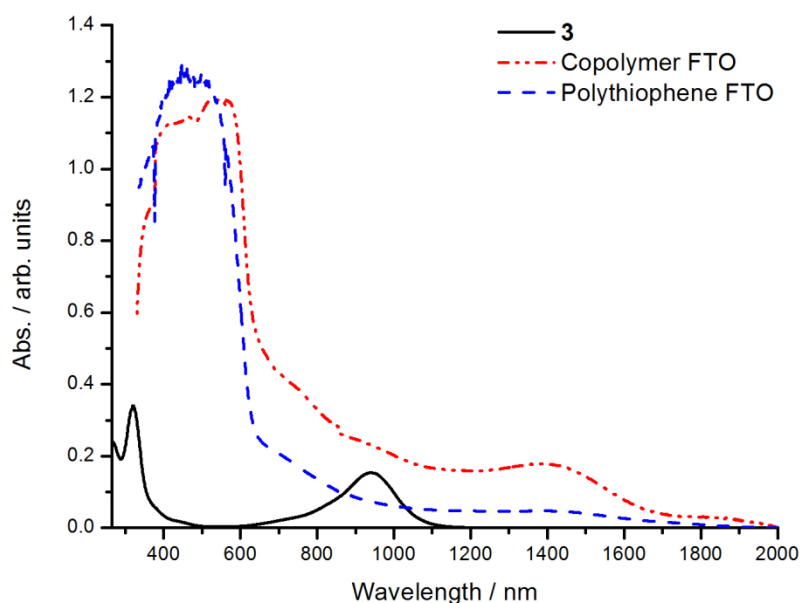
Figure 8. Normalised UV/Vis/NIR spectra of **3** in DMSO, a copolymer of **3** and thiophene on FTO and polythiophene on FTO. Spectra suggest incorporation of dithiolene units into the film and significant red-shifting of the low-energy transition.

Conclusions

We have prepared two novel asymmetric *bis*-1,2-dithiolene complexes containing a readily-tuneable auxiliary ligand (R$_2$pipdt) and a ligand with polymerisable thiophene groups attached at the 3-position (b-3ted). Both complexes have been structurally and electronically characterised and show that, by simple variation of the R group, the solid-state and electronic properties of such complexes can be controlled. Experimental data are supported by computation on isolated and solid-state models, and results suggest that the properties of analogous complexes may be accurately predicted by such techniques.

Cyclic voltammetry of both complexes displays three electrochemically reversible redox processes, including the formation of a stable cation, suggesting such complexes may be useful as ambipolar semiconductors for field-effect transistors. A negative solvatochromic response was shown in both complexes and therefore further investigation will look at the first hyperpolarisability (*β*) of such systems and the development of second-order NLO materials.

Electrochemical polymerisation of **3** has been shown to form a redox-active film, most likely through covalent linking of the thiophene groups. The electrochemical and spectroscopic properties of a poly-**3** coated platinum electrode confirm the incorporation of intact dithiolene units into a conducting film with redox processes

similar to that of the monomer. A co-polymer of **3** with thiophene showed strong absorption across the visible and NIR range, consistent with incorporation of the dithiolene units. Further work is required to fully characterise the structure of the polymers and to establish the extent to which an interplay between the conductive properties of the polythiophene backbone and the optical properties of the pendent dithiolene can be harnessed to yield characteristic and tuneable optical properties.

Experimental

Electrochemical experiments were performed in dry DMF (Sigma-Aldrich) or dry DCM (stored over KOH, distilled over P_2O_5) and solutions were degassed with N_2 before use. TBABF$_4$ was used as supporting electrolyte and was prepared from tetrafluoroboric acid and tetrabutyl ammonium hydroxide and recrystallised 5 times from water and dried under vacuum at 60°C for 2 weeks.

Cyclic voltammetry was performed at room temperature on a *ca*. 1 mM monomer solution in dry DMF using 0.1 M TBABF$_4$ supporting electrolyte in a three electrode cell. The working electrode was a 0.2 mm^2 Pt wire sealed in glass. The reference electrode was Ag/AgCl (sat. KCl), calibrated at +0.55 V against Ferrocene/Ferrocenium in the background electrolyte, and the counter electrode was a Pt rod.

Electrochemical polymerisation was performed at room temperature on a *ca*. 10 mM monomer solution in dry DCM using 0.3 M TBABF$_4$ as supporting electrolyte in a three electrode cell. The working electrode was a 387 mm^2 Pt disc, the reference electrode was Ag/Ag$^+$ (0.1 M AgNO$_3$), calibrated at +0.55 V against Ferrocene/Ferrocenium, and the counter electrode was a Pt gauze.

UV/Vis/NIR measurements were recorded in DMF using a quartz cell of path length 10 mm on a Perkin-Elmer Lambda 9 spectrophotometer, controlled by a datalink PC, running UV/Winlab software. OTTLE measurements were recorded in a cell of path length 0.5 mm using dry DMF and 0.1 M TBABF$_4$ as supporting electrolyte in a three electrode cell. The working electrode was a Pt/Rh gauze, the reference electrode was Ag/AgCl (sat. KCl) and the counter electrode was a platinum wire.

Geometry optimisations for isolated molecular units of **3** and **4** were carried out using the Gaussian 03 program,[31] utilising the X-ray crystallographic coordinates for the starting structures. The wavefunction was expanded using the Pople 6-31G* basis set for all atoms,[32, 33] coupled to the Becke three parameters hybrid exchange and the Perdew-Wang 1991 correlation functionals (B3PW91).[34, 35] Optimised structures were subsequently verified as minima on the potential energy surfaces by the absence of negative values in the frequency calculations. The molecular orbital isosurfaces were generated using the cubegen utility in Gaussian 03 and visualised using ArgusLab 4.0. TD-DFT calculations were carried out in the presence of the Tomassi polarisable continuum model (PCM) in a DCM solvation field,[36] with the first 70 singlet transitions

calculated. Simulated spectra were generated using Gausssum 2.1 freeware program, using a full-width half-maximum value of 3000 cm^{-1}.

Single-point energy calculations were undertaken using the CRYSTAL06[29] code to deduce the band structures for **3** and **4**, with the X-ray crystal structures providing the input models. Standard 6-31G** basis sets[37-39] were used throughout, while exchange and correlation were included by use of the B3LYP hybrid functional.[26] This method has been previously shown to give band dispersions and gap widths in good agreement with experiment for a wide range of materials.[40, 41] Calculations were terminated once the energy convergence fell below 10^{-6} au. Electronic band structures were sampled using a 4×4×4 Monkhurst-Pack mesh,[42] and subsequently visualised along with atom-projected densities of states plots.

[Ni(Bz$_2$pipdt)(b-3ted) (**3**)

To a stirred solution of sodium (13.4 mg, 0.583 mmol) in dry MeOH (10 ml) under a nitrogen atmosphere was added **1** (82.3 mg, 0.292 mmol) and the reaction mixture stirred for 1 hr. **2a** (85.8 mg, 0.292 mmol) and NiCl$_2$.6H$_2$O (69.4 mg, 0.292 mmol) were dissolved in MeOH (5 ml) and added to the reaction mixture. After 1 hour the crude product was filtered in air and washed with cold MeOH. The crude product was dissolved in DCM and passed through a silica plug. The solvent was removed yielding a green precipitate, which was recrystallised from DMF/Et$_2$O yielding the title compound as dark green needles (30.7 mg, 16%). δ_H (250 MHz; CDCl$_3$) 3.76 (s, 4H, H$_e$), 5.1 (s, 4H, H$_d$), 6.68 (dd, 2H, J = 5.0, 1.3 Hz, H$_c$), 7.16 (dd, 2H, J = 3.0, 1.3 Hz, H$_b$), 7.31 (dd, 2H, J = 5.0, 3.0 Hz, H$_a$), 7.34-7.52 (m, 10H, -Ph); MS (ESI) (*m/z*): 639 [M+1]$^+$. Anal calcd for C$_{28}$H$_{24}$N$_2$S$_6$Ni: C, 52.6; H, 3.8; N, 4.4. Found C, 52.2; H, 3.9; N, 4.1. λ_{max} = 940 nm (ε = 15.8x10^3 M^{-1}cm^{-1})

[Ni(^{i}Pr$_2$pipdt)(b-3ted) (**4**)

To a stirred solution of sodium (14.0 mg, 0.609 mmol) in dry MeOH (10 ml) under a nitrogen atmosphere was added **1** (85.8 mg, 0.304 mmol) and the reaction mixture stirred for 1 hr. **2b** (0.700 mg, 0.304 mmol) and NiCl$_2$.6H$_2$O (72.3 mg, 0.304 mmol) were dissolved in MeOH (5 ml) and added to the reaction mixture. After 1 hour the crude product was filtered in air and washed with cold MeOH. The crude product was dissolved in DCM and passed through a silica plug. The solvent was removed yielding a green precipitate, which was recrystallised from DMF/Et$_2$O yielding the title compound as dark green needles (28.3 mg, 17%). δ_H (250 MHz; CDCl$_3$) 1.32 (d, 12H, J = 6.6 Hz, H$_d$), 3.60 (s, 4H, H$_f$), 5.0 (m, 2H, H$_e$), 6.69 (dd, 2H, J = 5.0, 1.3 Hz, H$_c$), 7.13 (dd, 2H, J = 3.0, 1.3 Hz, H$_b$), 7.31 (dd, 2H, J = 5.0, 3.0 Hz, H$_a$); MS (ESI) (*m/z*): 543 [M+1]$^+$. Anal

calcd for $C_{20}H_{24}N_2S_6Ni$: C, 44.2; H, 4.4; N, 5.2. Found C, 44.5; H, 4.2; N, 5.2. λ_{max} = 928 nm (ε = 11.4x10^3 $M^{-1}cm^{-1}$)

X-ray crystallography

[Ni(Bz$_2$pipdt)(b-3ted)] (**3**) Dark green blocks (dimensions 0.57 x 0.23 x 0.12 mm) C_{28} H_{24} N_2 Ni_1 S_6, T = 150 K, space group P2$_1$/n, M_r = 639.62, monoclinic, a = 9.2735(3), b = 13.5383(4), c = 22.4070(7) Å, β = 91.326(2)°, V = 2812.39(15) Å^3, D_c = 1.511 Mg m^{-3}, μ = 1.157 mm^{-1}, no. of reflections for cell = 6682, θ_{max} = 29.546°, Z = 4, 22463 reflections collected, unique [R_{int}] = 7306 [0.054], T_{min}/T_{max} = 0.70/0.87, parameters 352, R_1 [$F > 4\sigma(F)$] = 0.0521, wR = 0.1355, $\Delta\rho_{max}/e$ Å^{-3} = 1.23, $\Delta\rho_{min}/e$ Å^{-3} = -0.91.

[Ni(^{i}Pr$_2$pipdt)(b-3ted)] (**4**) Dark green blocks (dimensions 0.29 x 0.28 x 0.10 mm) C_{20} H_{24} N_2 Ni_1 S_6, T = 150 K, space group P2$_1$/n, M_r = 543.53, monoclinic, a = 9.4169(2), b = 27.4559(7), c = 10.0584(2) Å, β = 114.9350(10)°, V = 2358.18(9) Å^3, D_c = 1.531 Mg m^{-3}, μ = 1.365 mm^{-1}, no. of reflections for cell = 7654, θ_{max} = 29.613°, Z = 4, 16512 reflections collected, unique [R_{int}] = 6040 [0.036], T_{min}/T_{max} = 0.68/0.87, parameters 262, R_1 [$F > 4\sigma(F)$] = 0.0440, wR = 0.1109, $\Delta\rho_{max}/e$ Å^{-3} = 0.77, $\Delta\rho_{min}/e$ Å^{-3} = -0.59.

References

[1] J. A. McCleverty, *Prog. Inorg. Chem.*, 1968, **10**, 49.

[2] J.-Y. Cho, B. Domercq, S. C. Jones, J. Yu, X. Zhang, Z. An, M. Bishop, S. Barlow, S. R. Marder and B. Kippelen, *J. Mater. Chem.*, 2007, **17**, 2642.

[3] P. Cassoux, *Coord. Chem. Rev.*, 1999, **185**, 213.

[4] N. Robertson and L. Cronin, *Coord. Chem. Rev.*, 2002, **227**, 93.

[5] U. T. Mueller-Westerhoff, B. Vance and D. I. Yoon, *Tetrahedron*, 1991, **47**, 909.

[6] J. Fabian, *Chem. Rev.*, 1992, **92**, 1197.

[7] S. Curreli, P. Deplano, C. Faulmann, A. Ienco, C. Mealli, M. L. Mercuri, L. Pilia, G. Pintus, A. Serpe and E. F. Trogu, *Inorg. Chem.*, 2004, **43**, 5069.

[8] S. M. Kuebler and R. G. Denning, *Chemical Physics Letters*, 1996, **250**, 120.

[9] C. Faulmann and P. Cassoux, *Prog. Inorg. Chem.*, 2004, **52**, 399.

[10] A. Vogler and H. Kunkely, *Angew. Chem., Int. Ed.*, 1982, **21**, 77.

[11] E. A. M. Geary, L. J. Yellowlees, S. Parsons, L. Pilia, A. Serpe, M. L. Mercuri, P. Deplano, S. J. Clark and N. Robertson, *J. Chem. Soc., Dalton Trans.*, 2007, 5453.

[12] C.-T. Chen, S.-Y. Liao, K.-J. Lin and J.-J. Lai, *Adv. Mater.*, 1998, **10**, 334.

[13] F. Bigoli, C.-T. Chen, W.-C. Wu, P. Deplano, M. L. Mercuri, M. A. Pellinghelli, L. Pilia, G. Pintus, A. Serpe and E. F. Trogu, *Chem. Comm.*, 2001, 2246.

[14] J. Roncali, *Chem. Rev.*, 1992, **92**, 711.

[15] C. Pozo-Gonzalo, R. Berridge, P. J. Skabara, E. Cerrada, M. Laguna, S. J. Coles and M. B. Hursthouse, *Chem. Comm.*, 2002, 2408.

[16] F. Wuerthener, *Angew. Chem. Int. Ed. Eng.*, 2001, **40**, 1037.

[17] T. Anjos, S. J. Roberts-Bleming, A. Charlton, N. Robertson, A. R. Mount, S. J. Coles, M. B. Hursthouse, M. Kalaji and P. J. Murphy, *J. Mater. Chem.*, 2008, **18**, 475.

[18] P. J. Skabara, C. Pozo-Gonzalo, N. L. Miazza, M. Laguna, E. Cerrada, A. Luquin, B. González, S. J. Coles, M. B. Hursthouse, R. W. Harrington and W. Clegg, *Dalton Trans.*, 2008, 3070.

[19] C. L. Kean, D. O. Miller and P. G. Pickup, *J. Mater. Chem.*, 2002, **12**, 2949.

[20] C. L. Kean and P. G. Pickup, *Chem. Comm.*, 2001, 815.

[21] S.-J. Roberts-Blemming, G. L. Davies, M. Kalaji, P. Murphy, A. M. Celli, D. Donati and F. Ponticelli, *J. Org. Chem.*, 2003, **68**, 7115.

[22] R. Isaksson, T. Liljefors and J. Sandstroem, *J. Chem. Res. (S)*, 1981, 43.

[23] F. Bigoli, P. Deplano, M. L. Mercuri, M. A. Pellinghelli, L. Pilia, G. Pintus, A. Serpe and E. F. Trogu, *Inorg. Chem.*, 2002, **41**, 5241.

[24] M. B. Hursthouse, M. E. Light and P. J. Murphy, Private Communication, RefCode: 216340 from CCDC, Editon edn., 2003.

[25] C. F. Macrae, P.R. Edgington, P. McCabe, E. Pidcock, G. P. Shields, R. Taylor, M. Towler and J. v. d. Streek, *J. Appl. Cryst.*, 2006, **39**, 453.

[26] R. J. Mortimer and N. M. Rowley, in *Comprehensive Coordination Chemistry II*, eds. J. A. McCleverty and T. J. Meyer, Elsevier-Pergamon, Oxford, Editon edn., 2004, vol. Vol. 9, pp. pp. 581-619.

[27] M. D. Ward and J. A. McCleverty, *J. Chem. Soc., Dalton Trans.*, 2002, 275.

[28] M.-F. Charlot and A. Aukauloo, *J. Phys. Chem. A*, 2007, **111**, 11661.

[29] R. Dovesi, V. R. Saunders, C. Roetti, R. Orlando, C. M. Zicovich-Wilson, F. Pascale, B. Civalleri, K. Doll, N. M. Harrison, I. J. Bush, P. D'Arco, M. Llunell, CRYSTAL06, University of Torino, Torino and 2006.

[30] A. R. Mount and M. T. Robertson, *Phys. Chem. Chem. Phys.*, 1999, **1**, 5169.

[31] M. J. Frisch, G. W. Trucks, H. B. Schlegel, G. E. Scuseria, M. A. Robb, J. R. Cheeseman, J. J. A. Montgomery, T. Vreven, K. N. Kudin, J. C. Burant, J. M. Millam, S. S. Iyengar, J. Tomasi, V. Barone, B. Mennucci, M. Cossi, G. Scalmani, N. Rega, G. A. Petersson, H. Nakatsuji, M. Hada, M. Ehara, K. Toyota, R. Fukuda, J. Hasegawa, M. Ishida, T. Nakajima, Y. Honda, O. Kitao, H. Nakai, M. Klene, X. Li, J. E. Knox, H. P. Hratchian, J. B. Cross, V. Bakken, C. Adamo, J. Jaramillo, R. Gomperts, R. E. Stratmann, O. Yazyev, A. J. Austin, R. Cammi, C. Pomelli, J. W. Ochterski, P. Y. Ayala, K. Morokuma, G. A. Voth, P. Salvador, J. J. Dannenberg, V. G. Zakrzewski, S. Dapprich, A. D. Daniels, M. C. Strain, O. Farkas, D. K. Malick, A. D. Rabuck, K. Raghavachari, J. B. Foresman, J. V. Ortiz, Q. Cui, A. G. Baboul, S. Clifford, J. Cioslowski, B. B. Stefanov, G. Liu, A. Liashenko, P. Piskorz, I. Komaromi, R. L. Martin, D. J. Fox, T. Keith, M. A. Al-Laham, C. Y. Peng, A. Nanayakkara, M. Challacombe, P. M. W. Gill, B. Johnson, W. Chen, M. W. Wong, C. Gonzalez and J. A. Pople, Editon edn.

[32] R. Ditchfield, W. J. Hehre and J. A. Pople, *J. Chem. Phys.*, 1971, **54**, 724.

[33] V. A. Rassolov, M. A. Ratner, J. A. Pople, P. C. Redfern and L. A. Curtiss, *J. Comp. Chem.*, 2001, **22**, 976.

[34] J. P. Perdew, J. A. Chevary, S. H. Vosko, K. A. Jackson, M. R. Pederson, D. J. Singh and C. Fiolhais, *Phys. Rev. B*, 1993, **48**, 4978(E).

[35] J. P. Perdew, K. Burke and Y. Wang, *Phys. Rev. B*, 1996, **54**, 16533.

[36] M. T. Cancès, B. Mennucci and J. Tomasi, *J. Chem. Phys.*, 1997, **107**, 3032.

[37] M. M. Francl, W. J. Petro, W. J. Hehre, J. S. Binkley, M. S. Gordon, D. J. DeFrees and J. A. Pople, *J. Chem. Phys.*, 1982, **77**, 3654.

[38] P. C. Hariharan and J. A. Pople, *Theoret. Chimica Acta*, 1973, **28**, 213.

[39] V. A. Rassolov, J. A. Pople, M. A. Ratner and T. L. Windus, *J. Chem. Phys.*, 1998, **109**, 1223.

[40] J. Muscat, A. Wander and N. M. Harrison, *Chem. Phys. Lett.*, 2001, **342**, 397.

[41] W. F. Perger, *Chem. Phys. Lett.*, 2002, **368**.

[42] H. J. Monkhorst and J. D. Pack, *Phys. Rev. B* 1976, **13**, 5188.